Multi-objective optimization of P2P energy trading for consumer–prosumer benefits and reliability improvement in LV distribution grids

Polat, Keysan; Ahmadi, Bahman; Ozdemir, Aydogan

DOI
10.1016/j.esr.2025.101980

Publication date
2025

Document Version
Final published version

Published in
Energy Strategy Reviews

Energy Strategy Reviews 62 (2025) 101980

Contents lists available at ScienceDirect

Energy Strategy Reviews

journal homepage: www.elsevier.com/locate/esr

Multi-objective optimization of P2P energy trading for consumer–prosumer benefits and reliability improvement in LV distribution grids

Keysan Polat [a], Bahman Ahmadi [b,*], Aydogan Ozdemir [c]

[a] Department of Electrical Engineering, Istanbul Technical University, Istanbul, Turkey
[b] Department of Electrical Sustainable Energy, Delft university of technology, Delft, Netherlands
[c] Department of Electrical and Electronics Engineering, Kadir Has University, Istanbul, Turkey

ARTICLE INFO

Handling Editor: Xi Lu

Keywords:
Power system planning
Low voltage distribution networks
Peer-to-peer energy trading
Transactive energy market
Multi-objective optimization
Load point reliability indices

ABSTRACT

Integrating distributed generation into the main grid requires the active participation of both consumers and prosumers, offering technical and financial benefits for all stakeholders. This study proposes a multi-objective optimization approach to enhance peer-to-peer (P2P) market operations within low-voltage distribution grids. It focuses on optimizing the placement of modular PV panels, maximizing prosumer profits, and refining P2P strategies. Key objectives include minimizing the payback periods for PV owners and reducing the average monthly energy costs for consumers. The Multi-Objective Advanced Gray Wolf Optimizer (MOAGWO) is used as the solution method. Operational scenarios are also compared from a consumer reliability perspective as an assessment metric. The methodology is applied to a 55-node European low-voltage test feeder across six scenarios. Results indicate that prosumer payback periods remain around eight years for up to four prosumers but increase with further installations. Average monthly energy costs for customers ranged from 653 *to* 1079. A quality assessment based on three multi-objective optimization metrics showed that MOAGWO and MOGWO yielded comparable performances.

1. Introduction

Traditionally, electrical distribution networks functioned as passive grids that connected consumers to supply points, fulfilling their electrical needs. These grids were designed based on historical data and focused on the worst operational conditions of the network, typically experienced during peak load times [1]. The emergence of distributed generation (DG) units, battery energy storage systems (BESS), and electric vehicles (EVs) has led to the concept of Active Distribution Networks (ADN) [2], offering several advantages, such as reducing power losses [3], improving voltage profiles [4], and enhancing reliability [5]. However, increased penetration of distributed energy resources (DERs) beyond a critical threshold can also lead to problems like voltage rises and reverse power flows within the network. Therefore, network planners need to carefully consider both the benefits and potential issues when connecting DERs, particularly in active low-voltage network planning [6,7].

One effective way to enhance prosumers' financial benefits in a low-voltage network with high DER penetration is by selling surplus energy to Distribution System Operators (DSOs) or neighboring consumers through the Transactive Energy Market (TEM). In [8], a prosumer segmentation and operating envelope strategy was proposed to jointly reduce system costs and maximize prosumer profit in local electricity markets, emphasizing the importance of adaptive market participation strategies. Since DSOs may limit the amount of energy a prosumer can supply during specific time intervals or within certain geographical areas, TEM becomes a more appealing option for distributed generation owners [9,10]. Transactive Energy (TE) is defined as a system of economic and control mechanisms that facilitates a dynamic balance of supply and demand across the electrical infrastructure, using value as a key operational parameter [11].

Qayyum et al. proposed an intelligent energy-sharing platform that focused on providing a time-sensitive trading plan and reducing the overall network energy cost [12]. In [13], a TEM structure was designed where the prosumers could negotiate with flexible load consumers during energy shortages caused by incorrect forecasts. Hua et al. proposed a blockchain-based platform for microgrid prosumers to trade excess energy [14]. Similarly, in [15], a blockchain-enabled P2P energy trading society was introduced, incorporating multi-scale flexibility services to improve transaction coordination and market trust. The authors in [16] presented a case study of a microgrid where prosumers with DERs and flexible loads participated in a real-time energy market. Zheng et al. proposed a control strategy to coordinate the DGs in ADNs

* Corresponding author.
E-mail addresses: keysan.polat@siemens.com (K. Polat), b.ahmadi@tudelft.nl (B. Ahmadi).

https://doi.org/10.1016/j.esr.2025.101980
Received 21 July 2025; Received in revised form 19 October 2025; Accepted 4 November 2025
Available online 15 November 2025

Nomenclature

AAOD	Average Annual Outage Duration
ADN	Active Distribution Network
ALPG	Artificial Load Profile Generator
AOD	Average Outage Duration
BESS	Battery Energy Storage System
DER	Distributed Energy Resource
DG	Distributed Generation
DisCo	Distribution Company
DSO	Distribution System Operator
DSUC	Distribution System Usage Charges
EV	Electric Vehicle
HV	Hyper-Volume
LV	Low-Voltage
MOAGWO	Multi-Objective Advanced Gray Wolf Optimizer Algorithm
MOGWO	Multi-Objective Gray Wolf Optimizer
MOMVO	Multi-Objective Multi-Verse Optimization
MV	Medium Voltage
NSGA-III	Nondominated sorting genetic algorithm III
P2P	Peer-To-Peer
PSC	Pareto Solution Candidate
PV	Photovoltaic
r	Average repair duration
SM	Spacing Metric
TE	Transactive Energy
TEM	Transactive Energy Market
λ	Failure rate

and optimize energy utilization and costs through peer-to-peer (P2P) trading in [17]. Two-level framework optimizing network-constrained P2P transactions among multiple microgrids under uncertainty is investigated in [18]. In [19], a demand-response-based multi-layer P2P trading framework was proposed for renewable-powered microgrids with EV integration, emphasizing adaptive flexibility in trading decisions.

To minimize costs and optimize resource scheduling, it is essential that systems can reliably and consistently meet users' energy needs [20]. Achieving optimal solutions through multi-objective optimization in ADNs is critical for balancing diverse and often conflicting goals, such as cost efficiency, reliability, and sustainability [21]. In the context of P2P energy trading, identifying the most cost-effective and efficient methods for generating, distributing, storing, and consuming energy is vital for minimizing system losses. Several studies have applied optimization algorithms to develop optimal energy management strategies for residential prosumers in P2P electricity markets and microgrids with DERs and flexible loads [22,23]. These studies aimed to minimize costs and optimize energy usage. A data-driven real-time operation strategy based on deep reinforcement learning for networked microgrids was also proposed in [24], emphasizing adaptive energy management under dynamic operating conditions. One proposed approach involves network-aware P2P energy sharing, which utilizes multi-objective optimization [25]. Additionally, a negotiation algorithm for DGs in retail markets has been suggested [26]. This algorithm supports self-management of energy trades and generates Pareto-optimal solutions through multi-objective optimization and a decision-making methodology.

Many studies on P2P energy trading have primarily focused on the technical and economic perspectives of either consumers or prosumers, often overlooking the benefits for all stakeholders [27–29]. For instance, [30] investigated short-term, scenario-oriented energy management that considers market interactions and end-user participation, but the balance between stakeholder benefits and constraints in P2P schemes under LV network constraints was not fully addressed. This study introduces a multi-objective optimization framework aimed at maximizing benefits for all stakeholders in a P2P energy trading market operating within a low-voltage (LV) distribution grid. In this context, the optimal placement of modular photovoltaic (PV) panels, the profits for prosumers, and the strategies for P2P market interactions between consumers and prosumers are determined. The goal is to minimize the payback period for PV owners while also reducing the average monthly energy costs for customers. The solution employs the Multi-Objective Advanced Gray Wolf Optimizer Algorithm (MOAGWO) [31]. Additionally, the study includes a reliability analysis comparing the load point reliability indices across various operational scenarios.

The main contributions of the paper are as follows:

- Pareto optimal solutions are identified to facilitate decision-making in balancing the conflicting goals of LV distribution grids and maximizing benefits for DSOs, consumers, and prosumers.
- A multi-objective framework for P2P energy trading is proposed, addressing various economic objectives and enhancing customer reliability.
- The payback period for PV owners and the average monthly energy costs for customers are optimized to encourage efficient resource utilization and the adoption of DERs.
- A strategic investment roadmap is provided to guide sustainable grid development, taking into account the effects of prosumer integration on load point reliability.
- Optimal locations for prosumers are determined using MOAGWO to ensure profit maximization and grid efficiency, thereby supporting targeted investment strategies.

The structure of the paper is as follows. The statement of the problem, including the objective functions and constraints, is described in Section 2. Section 3 is devoted to the MOAGWO method and its implementation for the multi-objective optimization problem. Section 4 shows the simulation results for test system applications. Finally, conclusions are summarized in Section 5.

2. Formulation of the multi-objective optimization problem

2.1. LV distribution network and P2P energy trading

The concept of transactive energy aims to facilitate a decentralized and efficient exchange of electricity between prosumers and consumers within a local electricity market. The key elements and principles that underlie transactive energy can be found in [32]. This market enables prosumers to actively participate, optimize their electricity usage and generation, and benefit from trading electricity with other market participants.

This study focuses on transactive energy trading in a low-voltage (LV) distribution grid consisting of residential loads. In this context, houses are classified into two categories: traditional houses without electricity generation facilities and prosumers equipped with rooftop generation units. Prosumers may generate surplus electricity beyond their own demand, which varies according to the time of day and weather conditions. They utilize their own generation as much as possible. In contrast, traditional houses can select suitable suppliers from neighboring prosumers or the Distribution Company (DisCo). Consumer preferences typically depend on energy prices and additional factors, such as environmental concerns, which can attract them to energy generated from renewable sources. Conversely, consumers may prefer the supply from the distribution grid, which they consider more reliable, often without regard to their own energy generation capabilities. Random and consumer-specific loyalty factors influence these consumer preferences.

Each prosumer offers a unique price to consumers, determined by the distribution system usage charges (DSUC) paid to the DisCo

for utilizing their infrastructure and the power losses incurred in the transmission from prosumers to consumers. The bidding price for each consumer is calculated using the following:

$$C_{\text{pv}} = C_{\text{opr}} + C_{\text{pf}} \tag{1}$$

$$B_{i,n} = \sum_{t=1}^{N_t} (E_{nt} + E_{lt,ni}) \cdot C_{pv} \cdot (1 + (C_{R_{it}}/100)) \tag{2}$$

where C_{pv} shows the base price of the prosumer, C_{opr} is the fixed distribution system usage cost per kWh, C_{pf} is the energy price per kWh that the DisCos will pay to the prosumers in the traditional market (based-on Turkey electrical regularities, it is considered to be half of the DisCo retail market prices). $B_{i,n}$ is the bidding price of ith prosumer for the nth consumer. E_{nt} and $E_{lt,ni}$ denote the energy need of the nth consumer at the tth time slot that is supposed to be supplied by the ith prosumer and the energy loss in the route connecting nth consumer to ith prosumer, respectively. $C_{R_{it}}$ is the profit rate of ith generation in the time interval t.

A detailed formulation of the objective functions based on the above discussion is elaborated in the following sections.

2.2. Objective functions

This study proposes a two-dimensional objective function: total energy cost and payback duration of PV units for the benefit of the consumers and prosumers, respectively.

2.2.1. Total energy cost (f_{EC})

The price of prosumer energy depends on the energy loss along the route between the prosumer and the load point. Therefore, each customer's bidding price will differ slightly in the same time interval. It should be considered that the lower price may not guarantee a bilateral contract between the prosumer and consumer as, based on the loyalty factor of the load point, it could be challenging to satisfy the expectations of the customer.

The energy cost for the consumers in the system can be calculated according to energy market specifications between prosumers, consumers, and the DisCo. As mentioned before, the energy price that a customer pays to a prosumer can be calculated based on $B_{i,n}$. This is true when a customer is willing to use prosumer energy, but for a general case, the equation can be modified as follows;

$$B_{n,i} = \begin{cases} B_{i,n}, & \text{if willing to use prosumer energy} \\ 0, & \text{if not willing to use prosumer energy} \end{cases} \tag{3}$$

where $B_{n,i}$ is the price that nth consumer should pay to ith prosumer. Note that the rest of the time intervals that the nth consumer will not be supplied by prosumers will use the energy from DisCo, and the cost for that can be modeled by $C_{n,DisCo}$.

The energy cost for each customer can be calculated using the equations mentioned earlier. The energy cost for all the consumers in the system is an objective function for the optimization process and can be calculated as:

$$f_{\text{EC}} = \sum_{n=1}^{N} \left(\left(\sum_{i=1}^{N_p} B_{n,i} \right) + C_{n,DisCo} \right) \tag{4}$$

where N is the total number of consumers in the system and N_p is the number of prosumers in the system.

2.2.2. PV payback time (f_{PB})

Based on the investment, operation, and maintenance costs of prosumers in the system and the income of each prosumer for the market type in this paper, we can estimate the payback time of the PV units. The investment, operation, and maintenance costs of prosumers (for PV units) can be calculated as follows;

$$C_{IOM} = \sum_{n=1}^{N_p} (\overline{IC}_{PV} + D \cdot \overline{O\&M}_{PV}) \times S_{PV_n} \tag{5}$$

where $\overline{IC}$ denotes a PV investment cost of a prosumer in USD/kW; whereas $\overline{O\&M}$ denotes the annual operation and maintenance costs of the units in USD/kW-yr and D represents the estimated lifetime duration of the PV units. S_{PV} is the size of PV units installed at the prosumer connection point.

The estimated annual income of prosumers can be calculated based on the amount of energy sold to consumers and DisCo ($C_{i,DisCo}$).

$$C_p = \sum_{n=1}^{N} \sum_{i=1}^{N_p} B_{n,i} + \sum_{i=1}^{N_p} C_{i,DisCo} \tag{6}$$

The payback time will be the ratio of PV lifetime cost to the annual income of the prosumer:

$$f_{\text{PB}} = \frac{C_{IOM}}{C_p} \tag{7}$$

2.3. Constraints

There are some physical and logical constraints that should be considered in the optimization process. Each load point that is a candidate to install a rooftop PV unit can accommodate only one PV unit (with a specified size). These PV units have limited generation capacities, and their total capacity cannot be greater than the peak load demand of the prosumer.

$$P_{\text{PV},t} \le S_{\text{PV}} \tag{8}$$

where $P_{\text{PV},t}$ is the PV output at time t.

According to market conditions, DisCos offer fixed prices for the prosumer surplus energy, which is much lower than the retail market prices. All TEM pricing rules in (2) are built with respect to this price, and therefore, the market limits the profit rate of the prosumer to make the overall prosumer bidding price lower than the distribution company price.

$$B_{i,n} \le C_{\text{ret}}, \forall\, i = 1, \dots, N_p,\ n = 1, \dots, N \tag{9}$$

where C_{ret} is the DisCo retail price (per kWh). Constraint (9) guarantees that a prosumer should offer a price that is always lower than the Disco retail price for the consumer.

Finally, the sum of the power injected into the network by the prosumers and the main grid is equal to the total loads and LV distribution losses.

2.4. Problem formulation

Using the objectives and constraints discussed in the previous subsection, the proposed multi-objective optimization can be formulated as follows:

$$\underset{w.r.t. \quad \vec{X}}{\text{minimize}}\ F(\vec{X}) = \{f_{\text{EC}}, f_{\text{PB}}\} \tag{10}$$

$$\vec{X} = \{\vec{L}, \vec{C_R}, \vec{M}\}$$

$$Subject\ to \begin{cases} g_\mu \ge 0, & \mu = 1, 2, \dots, p \\ h_\phi = 0, & \phi = 1, 2, \dots, q \end{cases}$$

where $\vec{L}$ is a common location vector for LV modular rooftop PV units, $\vec{C_R}$ is the control variable vector for prosumer profits, and $\vec{M}$ is the control variable for P2P market strategy. The terms h_ϕ and g_μ denote the ϕth equality and μth inequality constraints, respectively. Note that f_{EC} and f_{PB} are the conflicting objectives in the problem.

3. Solution methodology

3.1. Multi-objective optimization problems

The mathematical formulation of a K-dimensional multi-objective optimization problem can be expressed as follows:

$$\underset{w.r.t. \quad \vec{X}}{\text{minimize}} \; F(\vec{X}) = \{f_1(\vec{X}), f_2(\vec{X}), \ldots, f_K(\vec{X})\} \tag{11}$$

$$\vec{X} = \{\mathbf{x}_1, \mathbf{x}_2, \ldots, \mathbf{x}_d\}$$

$$Subject \quad to \begin{cases} g_\phi(\vec{X}) \geq 0, \phi = 1, 2, \ldots, p \\ h_\mu(\vec{X}) = 0, \mu = 1, 2, \ldots, q \\ (\vec{X})^{lb} \leq \vec{X} \leq (\vec{X})^{ub} \end{cases}$$

A set of solutions can be found for K individual objective functions and d control variables as an acceptable trade-off instead of an optimal solution. Note that $(\vec{X})^{lb}$ and $(\vec{X})^{ub}$ denote the lower and the upper bound vectors of the control variable vector $\vec{X}$, respectively. The optimal solutions can be characterized by dominance relations, Pareto efficiency, and optimality definitions [33].

3.2. Multi-objective advanced gray wolf algorithm (MOAGWO)

MOAGWO is the adoption of the AGWO method for multi-objective optimization problems. It is already shown in [31] that the AGWO algorithm would improve the simulation speed and convergence of the GWO algorithm [34]. The basic idea was to apply a dynamic method to evaluate the wolf positions, either in the exploration or the exploitation phase. Additionally, the mirroring distance concept was used to update the search agents' positions, ensuring that the positions remained within the feasible range [31].

A brief explanation of the search process in the MOAGWO is as follows. Each wolf in the AGWO-based optimization process is called an agent, and the positions of the agents are shown by $\vec{X}$. The positions of the agents at itth iteration are shown by $\vec{X}_{it}$. Based on the objective functions for the optimization process, each agent has a set of objective values ($F(\vec{X})$). The best agents will be selected and stored in a set consisting of leaders. The positions of each leader are shown by $\vec{X}_l$ and the corresponding set of objective values by $F_l(\vec{X})$. Note that in MOAGWO, the group of wolf agents includes N_w agents.

The mathematical formulations for updating the positions of the agents in MOAGWO are as follows. The exploration or exploitation phase of the method is determined by the exploration rate (ER) using the following expression.

$$\text{ER} = b_1 - b_2 \times \frac{\text{it}}{\text{Max-it}} \tag{12}$$

where Max-it is the maximum iteration number. Note that the initial ER value is b_1 and it decreases with the increasing iterations and finally becomes $b_1 - b_2$ at the end of the optimization cycle. Since the ER is high at the beginning of the optimization process and low in the final iterations, the search agent's positions are assessed to be updated through the exploration phase in the early iterations compared to the final iterations. The evaluation of the position for each agent affected by the ER value is as follows:

$$\vec{X}_{it} = \begin{cases} \vec{X}_{it} & r_1 \geq ER \\ \vec{X}_{rand} & r_1 < ER \end{cases} \tag{13}$$

where r_1 is a random number between 0 to one and $\vec{X}_{rand}$ is a random position for the agent.

The three random non-dominated leaders at each iteration are selected from the set of leaders, which are renamed as α, β, and δ leaders in the algorithm. Depending on the exploration or exploitation phase of evaluation for each agent, the position of the agent will be updated as follows:

$$\vec{X}_{it+1} = \begin{cases} \frac{\vec{X}_1 + \vec{X}_2 + \vec{X}_3}{3} & r_2 \geq ER \\ \begin{cases} \vec{X}_4 & r_3 < 0.5 \\ \vec{X}_5 & r_3 \geq 0.5 \end{cases} & r_2 < ER \end{cases} \tag{14}$$

where r_2 and r_3 are a random number in between zero to one and $\vec{X}_1$ to $\vec{X}_5$ are defined as:

$$\vec{X}_1 = \vec{X}_\alpha - \vec{A}_1 \cdot |\vec{C}_1 \cdot \vec{X}_\alpha - \vec{X}_{it}| \tag{15}$$

$$\vec{X}_2 = \vec{X}_\beta - \vec{A}_2 \cdot |\vec{C}_2 \cdot \vec{X}_\beta - \vec{X}_{it}| \tag{16}$$

$$\vec{X}_3 = \vec{X}_\delta - \vec{A}_3 \cdot |\vec{C}_3 \cdot \vec{X}_\delta - \vec{X}_{it}| \tag{17}$$

$$\vec{X}_4 = \vec{X}_t + \vec{A}_4 \cdot |\vec{C}_4 \cdot \vec{X}_\alpha - \vec{X}_{it}| \tag{18}$$

$$\vec{X}_5 = \vec{X}_t + ((2 \cdot a \cdot \vec{r}_4 - a) \cdot cos(2\pi \vec{r}_5)) \cdot |\vec{C}_5 \cdot \vec{X}_\alpha - \vec{X}_{it}| \tag{19}$$

where $\vec{X}_\alpha$, $\vec{X}_\beta$, and $\vec{X}_\delta$ are the α, β, and δ position vectors for selected leaders and the other parameters are defined as:

$$\vec{A} = (2 \cdot a \cdot \vec{r}_6 - a) \cdot sin(2\pi \vec{r}_7) \tag{20}$$

$$a = 2 - 2 \times \frac{it}{\text{Max-it}} \tag{21}$$

$$\vec{C} = 2 \cdot \vec{r}_8 \tag{22}$$

where r_4 to r_8 are random vectors between zero and one.

After updating the positions of each agent, the corresponding set of objective function values ($F(\vec{X}) = \{f_1, \ldots, f_n\}$) is calculated for the agents. The best agents are selected based on the non-domination concept and stored in a repository called the "Archive" set. The non-dominated agents can be selected based on three possibilities for any two agents ($F_a(\vec{X})$ and $F_b(\vec{X})$); agent a may dominate agent b, b may dominate a, or neither a nor b dominates the other one based on the dominance definition given below.

Definition 1. Dominance: The agent a dominates b, if:

$$\forall m\{1, 2, 3, \ldots, w\}, \left[f_{a,m} \geqslant f_{b,i}\right] \wedge \left[i \in 1, 2, 3, \ldots, w : F(\vec{X})\right] \tag{23}$$

The next step updates the Archive by adding the non-dominated agents. The MOAGWO uses the crowding distance, a parameter that measures the distance between non-dominated agents, to remove dominated leaders from the archive and control the number of non-dominated leaders. It can allow the new non-dominated agent to be added to the Archive either by updating or removing some leaders when the set becomes full. Note that the maximum number of solutions in the Archive is N_{arch}. This process is briefly explained as follows:

- The new agent is not added to the Archive if at least one leader exists in the Archive and can dominate it.
- The new agent is added to the Archive if it dominates any leader, and the corresponding leader is therefore removed.
- This new agent is added to the Archive set if the new agent does not dominate any non-dominated leader in the set.
- In the case that the Archive set reaches its capacity and a new agent needs to be added, the grid mechanism [33] is used to reorganize the Pareto space and remove a leader in the most crowded segment.

The process continues to update the positions of the agents with respect to the positions of the leaders and update the Archive with better quality non-dominated solutions. A dynamic stop standard is added to MOAGWO to find more accurate Pareto solutions based on the Hyper-volume (HC) index [33]. The optimization process stops when the index is smaller than the pre-specified values. The mathematical formulation of the stopping criteria is given in Eq. (24).

$$B_{stop} = \begin{cases} \text{stop} & if \quad |HV(it, it-a)| < \epsilon \\ \text{next iteration} & otherwise \end{cases} \tag{24}$$

where B_{stop} is used for the stopping process, ϵ is a pre-specified small number denoting a tolerance, n and a are the current iteration number and a predefined integer value for the comparison of the solutions with HV index. The MOAGWO algorithm is shown in Algorithm 1.

Algorithm 1: MOAGWO algorithm

```
Give the algorithm parameter and population parameters;
Initialize the random population of agents (control variables X⃗);
Initialize the random population of leaders in the Archive
  repository;
while it ≤ Max-it do
    Check the boundaries of the agent using the mirroring
      method [31];
    Use the position of each agent to calculate the objective
      values (F(X⃗));
    Find the non-dominated agents;
    Update the Archive by non-dominated agents ;
    for each agent do
        Chose the exploration or exploitation phase;
        Select three random leaders from the Archive;
        Update X⃗ using the proposed formulations in [31];
    end
    Check the stopping criteria;
end
Return the Archive;
```

3.3. Reliability analysis and methodology implementation

Load point reliability indices are used as the decision criterion of Pareto optimal solutions. The load clustering details and details of reliability indices calculations with Monte Carlo Simulations can be found in [35,36].

The flowchart of the MOAGWO implementation for the problem defined by Eq. (10) is shown in Fig. 1. Note that $Q = \sum MTTF_{e,k} + \sum MTTR_{e,k}$ and Max_e is defined as the total number of equipment in the network. MTTF represents Mean Time to Failure, MTTR is Mean Time to Repair, and Max_e is the maximum number of components in the grid.

4. Results and discussion

4.1. Test system and data

European LV test feeder [37] is used as the test system in this study. There are 55 load points in this network, which are fed through 10 different line types, each having different characteristics. This network is connected to the 11 kV MV grid through an 800 kVA MV/LV transformer. The feeder is a three-phase radial network operating at a 416 V/50 Hz line voltage and connected to the 11 kV MV grid through an 800 kVA MV/LV transformer.

Each load point in this network has a separate load profile generated by using the Artificial Load Profile Generator (ALPG) [38]. The detailed information about the number of adults and children living in households and publicly available statistics for the devices and electric power consumption [39] was used in ALPG to generate near-accurate predicted energy consumption profiles. The load profile data can be find [38] and the load duration curves of the system and a random house for 365 days are shown in Fig. 2(a) and (b), respectively.

Table 1
Dis-Co energy price for different time intervals.

	Time interval	Price ($cent/kWh)
Day	06:00–17:00	12.6502
Peak	17:00–22:00	18.5386
Night	22:00–06:00	7.9413

Table 2
Reliability data of the LV distribution system.

	Failure rate (failure/year km)	Repair time (h)
Main feeder	0.001	4
Branches	0.001	2
Main supply	1	5

Real yearly data comprising the sun irradiation values of a specific area in Turkey are used in the optimization process [31]. The capacity factors of the PV units are selected to be 33%. In this study, we considered modular PV panels of 4 kW per prosumer, which are appropriate for a residential area comprising similar houses. The data of the generated power by prosumers can be found in [38] and the average output for the data of PV units is shown in Fig. 3. Optimal prosumer locations are identified as part of the multi-objective optimization process using the MOAGWO metaheuristic, which handles both discrete and continuous decision variables.

The load points are divided into three zones. Each zone is connected to other zone/s through a line segment. A random load point loyalty factor between 0.5 to 0.85 is assigned to each load point. This loyalty factor symbolizes consumer preferences between different prosumers and distribution companies based on environmental issues and adherence to traditions. Each consumer prefers using the prosumer energy if the prosumer offers a price less than the Dis-Co price multiplied by the loyalty factor.

The European LV test feeder comprises ten branch types with different cross-sections (unit length resistances) that will affect the active power losses. A matrix (**L**) is constructed to represent the line losses between the consumer–prosumer pairs for a unit (1 kW) of energy consumption. Total energy loss along the route from prosumer-i to consumer-n at time-t, $E_{lt,ni}$, can be computed as.

$$E_{lt,ni} = l_{in} \times E_{nt} \tag{25}$$

where l_{in} is the entry of L corresponding to prosumer-i and consumer-n, and E_{nt} denotes the energy consumption of consumer-n at time-t.

DisCo prices for residential consumers for the three time intervals are illustrated in Table 1 [40]. The price that Dis-Co pays for the prosumer supply is supposed to be half of these timely prices. In order that the prosumers can compete with the DisCo prices, they use two different C_{Rit}, considering the sunlight duration, one for normal daytime and the other for peak load duration.

Failure rate (λ) and average repair duration (r) of the cables extracted from the annual report of Istanbul Distribution Company-Trace District [41] are illustrated in Table 2 (see Fig. 4).

4.2. Simulation results

4.2.1. Optimization results

The Pareto optimal solutions of the constrained optimization problem formulated by Eq. (10) are obtained for six scenarios, each representing a different number of prosumers. For each scenario, optimal prosumer locations, prosumer profits, and P2P energy market strategy are determined for the two objectives. The Pareto fronts determined by the MOAGWO method for the six scenarios are shown in Fig. 5.

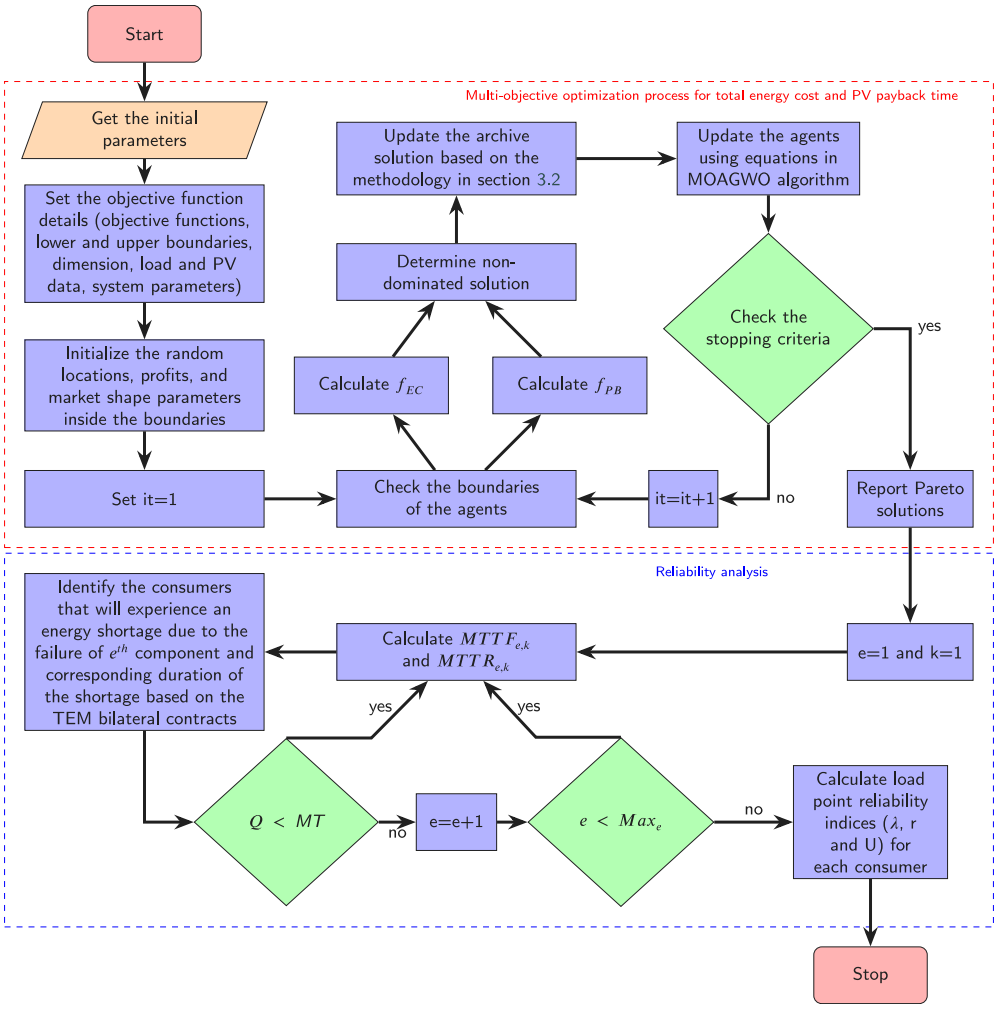

Fig. 1. The flowchart of the process.

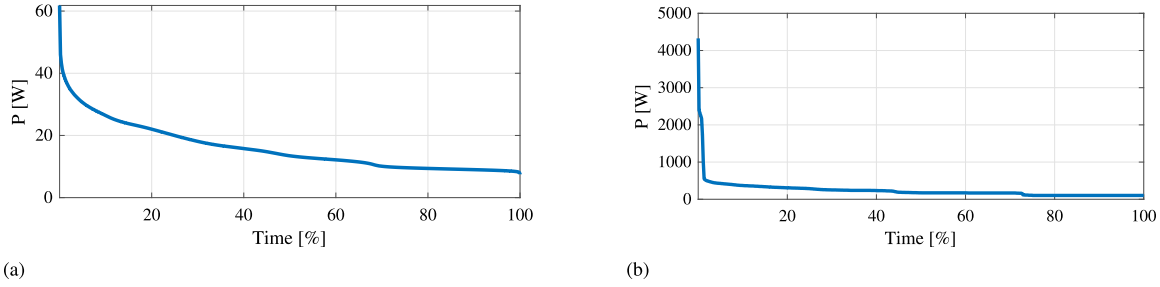

Fig. 2. Load duration curves for the system (a) and a random house (b) over 365 days.

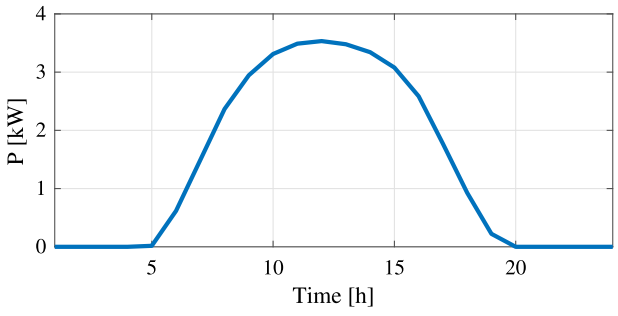

Fig. 3. The PV output curve.

The results show that the average payback duration for the prosumers is around eight years, up to 4 prosumers, and increases beyond this point. The non-dominated solutions derived from Fig. 6 indicate that one of the first four scenarios can be the best solution, depending on the intended payback duration.

The first scenario involves the optimal allocation of 1 PV unit. The best locations for that unit are found to be L14, L15, L16, L17, and L19, all in Zone-2 of the test system. The distribution of the prosumer profits ($\vec{C}_R$) for a day and peak periods are found as 5 to 150% with an average of 71.2% and 44 to 110% with an average of 71.8%, respectively. Optimal market strategies are provided in the Appendix for some specific Pareto solutions.

The Pareto solutions for the second scenario comprise two optimal PV locations. The first ones are in Zone-3 (L50, L51, L52, and L55),

Table 3
The percentage of prosumer profits from P2P transactions compared to DISCO prices for the Pareto Solutions of each scenario.

	PV-1		PV-2		PV-3		PV-4		PV-5		PV-6	
	Profit		Profit		Profit		Profit		Profit		Profit	
	Day	Paek	Day	Paek	Day	Paek	Day	Paek	Day	Paek	Day	Paek
sc-1	5–150	44–110										
sc-2	12–143	29–73	12–143	33–130								
sc-3	9–136	5–117	7–138	6–133	8–141	6–77						
sc-4	5–124	11–66	9–136	5–61	8–142	21–104	7–147	31–125				
sc-5	9–150	13–145	6–140	6–109	6–148	6–87	6148	7–148	6–136	7–126		
sc-6	5–149	5–150	5–146	5–144	5–150	5–147	5–146	6–148	5–149	6–149	5–150	7–115

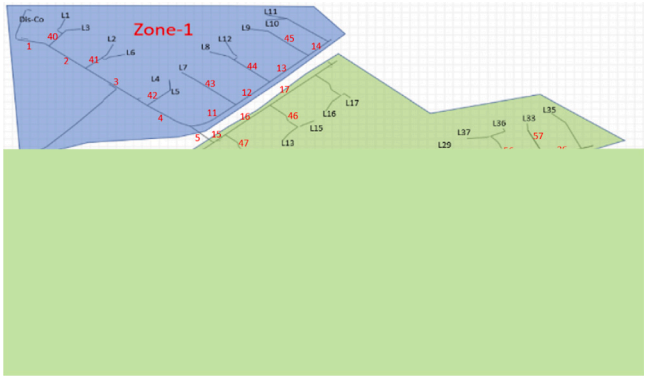

Fig. 4. European LV test feeder.

and the second ones are in Zone-2 (one from the L14-L18). Prosumer profits for the Day period are found to be 12%–143% and 13%–140% for the PV units in the third and second zones, respectively. For the Peak period, the profits are found as 29%–73% and 33%–130% for the prosumers in zones-3 and Zone-2, respectively. The profit ranges of the prosumers for the other scenarios are shown in Table 3, where the optimal PV locations in the Pareto solutions are not reported as they are spread all over the system. Optimal market strategies are again provided in the Appendix for some specific Pareto solutions.

The comparison of the control parameters and corresponding cost functions of different scenarios is done for some representative Pareto solution candidates (PSCs). For this purpose, two costs (670 and 780 $/month) and one PB duration (9 years) are selected as the reference parameters. Note that these references are selected at an appropriate part of the Pareto solution space where a solution exists for all scenarios. The three reference values in the Pareto space are shown in Fig. 6.

The optimal market strategies for the PCSs above are shown in the Appendix, where the optimal PV locations are shown on the right-hand side of each figure. These figures show the best consumer/prosumer pairs (contracts) for optimizing multiple objectives. Note that the optimum market strategy is shown for a specific random day of the year. The strategy for different days may change depending on the load and PV output profiles. These strategies show that the prosumers can supply all the consumers during the daytime once the number of prosumers in the system reaches four, indicating the best number of prosumers in the network and highlighting the grid's PV-hosting capacity. Moreover, any surplus energy generated is fed into the main grid at a predetermined base price, thereby extending the payback period.

4.2.2. Reliability results

In the second phase of the study, the load point reliability indices are calculated for each scenario. For the sake of simplicity, the same PSCs with constant objective function values (f_{PB} = 9 years, f_{EC} = 670 $/month f_{EC} = 780 $/month) are considered for each scenario. Therefore, there are 3 × 6 = 18 TE market cases and one traditional market case (base case without any prosumers) that will be considered in this section.

The P2P energy supply of a consumer depends on the irradiation level during the day, which is given in Fig. 3. Sometimes, more may be needed to supply a consumer or even meet the internal demand of the prosumer itself. Therefore, reliability analysis is performed considering both the irradiation level and the TE market strategy. In this regard, the TE transfer mechanism can provide energy in specific time intervals, as seen in the market strategy figures in the Appendix. For a downstream consumer with a bilateral contract with a prosumer, the failure duration is divided into time segments, each corresponding to either load fed or load loss. On the other hand, a downstream consumer without any bilateral contract with the prosumers will be subjected to an energy shortage along the total failure duration. Finally, upstream consumers will not be affected by the branch failures.

Load point reliability indices are calculated using the data in Table 2 and the procedure explained in Section 3.3 for the six scenarios for the specified PSCs. Figs. 7, 8(a), and (b) show the failure rate, average outage duration, and annual outage duration (λ, r, and U) for several cases, respectively. The Failure Rate, Average Outage Duration (AOD), and Average Annual Outage Duration (AAOD) for the BC scenario are 1.13 f/year, 4.25 h, and 4.79 h/year, respectively. It is clear from the figures that all three load point reliability indices show a steep decrease with increasing PV units up to sc-4, then they decrease with a lower slope or even slightly increase for sc-6.

Load point reliability improvements with respect to BC where all the load points are fed from the main grid through an MV/LV transformer, are illustrated in Tables 5–6. The average improvements provided by a single prosumer in failure rate, average outage duration, and annual outage duration are 6.0%, 5.8%, and 10.1%, respectively. An additional prosumer increases the improvements to 12.5%, 11.0%, and 20.6%. The third prosumer increases the improvements to 16.2%, 14.4%, and 26.8%. The results show that the highest incremental improvements in reliability indices are obtained for the first and the second PV units. The third and fourth units provide relatively less improvement, while the reliability contribution of the fifth and sixth units becomes negligible as the consumers who will prefer buying their energy from the prosumers go into saturation. This is an expected case since reliability is not included in the optimization process as an objective or constraint.

The total energy cost for the base case operation scenario is calculated as 1080 $/month. Table 7 shows the impact of each additional PV unit on load point reliability indices in %, total energy costs in USD/month, and payback duration in years for the selected PCSs. The notation sc-X/sc-Y denotes the relative improvements of the sc-X scenario with respect to the sc-Y scenario. FRI, AODI, and AAODI stand for Failure Rate Improvement, Average Outage Duration Improvement, and Annual Average Outage Duration Improvement, respectively. PBDI and ECI denote the improvements in two econometric indices, payback duration, and energy cost, respectively. Note that PBDI for SC-1/BC denotes the PBD of SC-1 since there is no prosumer in the base case operating conditions.

While energy cost, service quality, and reliability indices are important for consumers, the two important decision-making indices for the investors and prosumers are the payback duration of their investment

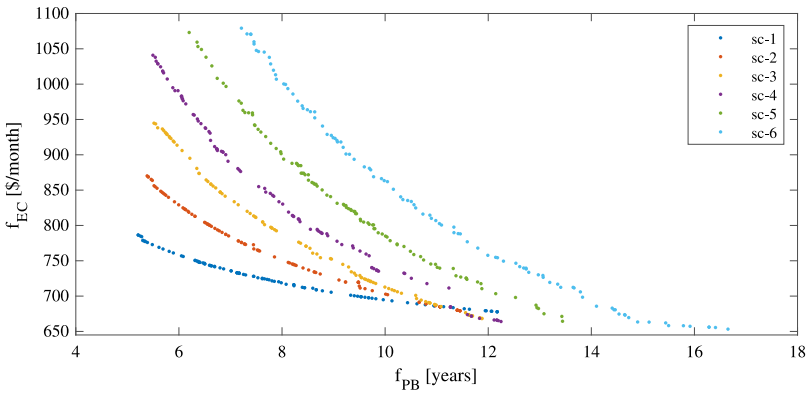

Fig. 5. Pareto optimal solutions for the six scenarios.

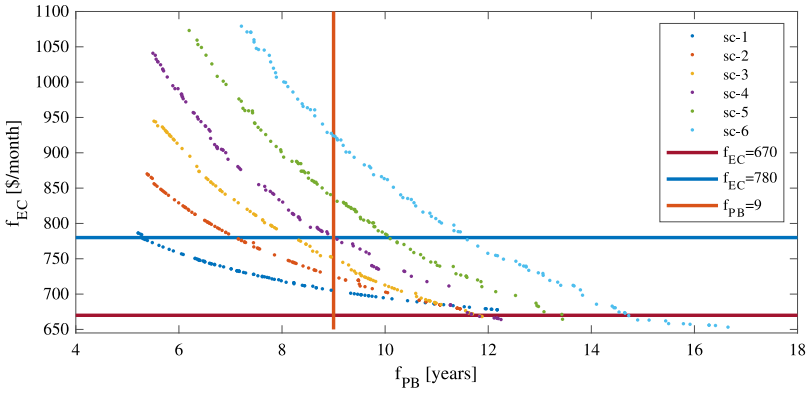

Fig. 6. Non-dominated Pareto optimal solutions for the six scenarios, reference costs, and reference payback duration.

Table 4
Failure Rate Improvement compared to BC (%).

	f_{PB} = 9	f_{EC} = 670 $/month	f_{EC} = 780 $/month
sc-1	5.7%	6.1%	6.2%
sc-2	12.5%	12.9%	12.0%
sc-3	16.3%	16.1%	16.3%
sc-4	21.3%	20.1%	21.4%
sc-5	24.3%	22.7%	23.6%
sc-6	23.7%	25.6%	25.5%

Table 5
AAOD Improvement compared to BC (%).

	f_{PB} = 9	f_{EC} = 670 $/month	f_{EC} = 780 $/month
sc-1	9.6%	10.3%	10.4%
sc-2	20.6%	21.3%	19.8%
sc-3	26.9%	26.7%	26.9%
sc-4	35.3%	33.6%	36.4%
sc-5	40.2%	37.8%	39.2%
sc-6	39.5%	42.4%	42.3%

Table 6
AOD Improvement compared to BC (%).

	f_{PB} = 9	f_{EC} = 670 $/month	f_{EC} = 780 $/month
sc-1	5.5%	6.0%	6.0%
sc-2	11.0%	11.4%	10.6%
sc-3	14.3%	14.5%	14.3%
sc-4	19.1%	18.4%	20.5%
sc-5	21.6%	20.4%	21.1%
sc-6	21.2%	22.8%	22.7%

and energy cost. Table 7 shows the impact of each PV unit on load point reliability indices, total energy cost, and payback duration. For a constant payback duration of 9 years, each additional prosumer improves the consumer reliability beyond the last one. However, the improvement rate is different. On the other hand, although the energy cost is less than the base case for all scenarios, the first prosumer provides a considerable decrease in the energy cost, but each of the subsequent ones brings an increase with respect to sc-1. The worst case is sc-6, where the consumers need to pay more even for a less reliable (more outages with longer durations) energy supply.

For constant energy cost (f_{EC} = 670 USD/month, f_{EC} = 780 USD/month) conditions, each new prosumer provides an improvement in reliability indices. However, the improvement rates get smaller with the increase in the number of prosumers. However, most of the additional units increase the payback duration, which demotivates the PV installation (see Table 4).

4.2.3. Quality of Pareto solutions

The quality of the Pareto solutions found by MOAGWO is verified by comparing them with the Pareto solutions obtained by Multi-Objective Multi-Verse Optimization (MOMVO) [42], Multi-Objective Gray Wolf Optimizer (MOGWO) [43], and Nondominated sorting genetic algorithm III (NSGA-III) [44]. For this purpose, three popular multi-objective optimization metrics, namely the Spacing Metric (SM), C metric, and Hyper-Volume (HV) metrics, are used. The details of the metrics can be found in [33].

As MOGWO, MOMVO, and MOAGWO are parameter-free algorithms, the NSGA-III parameters are first optimized with respect to the C metric across different parameter settings before the performance comparisons. The best parameters for the NSGA-III method are found as follows: Cross-over probability: 0.9; Mutation probability: 0.1; Cross-over factor: 20; Mutation factor: 20. Note that all the parameters are

Table 7
Impact of PV units on load point reliability indices, total energy cost and payback duration.

		sc-1/BC	sc-2/sc-1	sc-3/sc-2	sc-4/sc-3	sc-5/sc-4	sc-6/sc-5
f_{EC} = 670 $/month	FRI	6.11%	6.75%	3.27%	3.98%	2.61%	2.86%
	AODI	5.96%	5.46%	3.04%	3.92%	2.01%	2.39%
	AAODI	10.31%	10.96%	5.45%	6.91%	4.18%	4.58%
	PBD	12.1	−0.7	0.4	−0.2	1.8	1.2
f_{EC} = 780 $/month	FRI	6.16%	5.80%	4.33%	5.08%	2.22%	1.90%
	AODI	5.99%	4.61%	3.73%	6.16%	0.57%	1.63%
	AAODI	10.37%	9.40%	7.14%	9.49%	2.77%	3.12%
	PBD	5.3	1.4	1.6	0.8	1	1.5
f_{PB} = 9 year	FRI	5.68%	6.79%	3.82%	5.03%	2.95%	−0.52%
	AODI	5.53%	5.46%	3.34%	4.80%	2.42%	−0.39%
	AAODI	9.57%	10.99%	6.34%	8.42%	4.88%	−0.73%
	ECD	−375.6	17.3	29.7	33.0	45.9	92.9

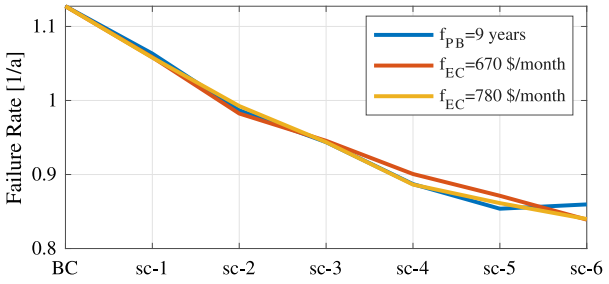

Fig. 7. Failure rate for each scenario.

Table 8
Optimization and simulation parameters for the optimization algorithms used.

Parameter	Value/Description
Algorithm type	MOGWO, MOMVO, MOAGWO (parameter-free); NSGA-III (parameter-based)
Cross-over probability (NSGA-III)	0.9
Mutation probability (NSGA-III)	0.1
Cross-over factor (NSGA-III)	20
Mutation factor (NSGA-III)	20
Maximum archive size	100
Maximum number of iterations	2500
Population size	25 (wolves, universes, or individuals depending on algorithm)
Stopping criteria parameters	$a = 60$, $\epsilon = 0.05$

optimized by experimental trials, and NSGA-III parameters are determined based on a grid-based experimental search. Other parameters, such as maximum archive size and the maximum number of iterations, are set to 100 and 2500, respectively. The search agent population size (also known as the number of wolves for MOGWO, the number of universes for MOMVO, and the number of individuals for NSGA-III) is set to 25. Note that for the stopping criteria of the optimization process, a is set to 60 and ϵ is set to 0.05. All algorithms are executed 100 times independently to account for stochastic variation, and the best Pareto results are reported. The same initialization strategy and objective function evaluation procedures are applied across all algorithms to guarantee consistency. We run the algorithms on a PC with 16 GB of RAM, an Intel Core i7-7700 3.6 GHz processor, and MATLAB version 2021b. The optimization and simulation parameters for the optimization algorithms used in this study are summarized in Table 8.

- The spacing metric:

The concept of SM has a long history in the field of multi-objective optimization. The SM evaluates the distribution of non-dominated solutions in the Pareto front space by calculating the standard deviation of the minimum Euclidean distances between the solutions. In other words, the SM uses a relative distance measure to assess how evenly the solutions are distributed along the Pareto front. This metric is useful for understanding the diversity of solutions in a given set and can be used to compare different sets of solutions in terms of their spread or dispersion. The formulation for the SM is as follows:

$$SM = \sqrt{(n(n-1))^{-1} \sum_{i=1}^{n} \sum_{j=1}^{n} (ED(i,j) - \overline{ED})^2} \quad (26)$$

where SM is the value of the spacing metric, $ED(i,j)$ is the Euclidean distance between non-dominated solutions i and j. $\overline{ED}$ is the mean distance between all pairs of solutions and n is the number of non-dominated solutions.

A lower SM value generally indicates a more evenly distributed set of solutions, whereas a higher value may indicate a more concentrated set.

The results of the SM for different multi-objective optimization algorithms are presented in the form of box plots in Fig. 9. It is important to note that each box plot represents the distribution of SM values obtained from 100 independent runs of each algorithm for each scenario of the study. This means that the box plots show the range, median, and interquartile range of the SM values for non-dominated solutions found for all six scenarios using each algorithm. By analyzing the box plots, we gain clear insight into the diversity and distribution of solutions generated by the MOAGWO algorithm. As shown in the figure, the SM values for MOAGWO, MOGWO, and MOMVO are very close to each other, and the NSGA-III method performs worst in terms of SM values.

- The C index:

The C-index is a measure of the diversity and distribution of solutions in a set of non-dominated solutions. It is calculated by finding the percentage of solutions in one set (A) that are dominated by at least one solution in another set (B). The C index can be calculated using the equation: $C(A,B) = \frac{|b \in B; \exists a \in A : a \preceq b|}{|B|} \times 100$, where a and b are the non-dominated solutions in sets A and B determined by two different methods, respectively. It is important to calculate both $C(A,B)$ and $C(B,A)$ in order to fully understand the dominance of the solutions in each set. A higher value of $C(B,A)$ compared to $C(A,B)$ indicates a more acceptable convergence of the solutions in set A.

Based on the results shown in Table 9, it appears that the method MOAGWO produces a set of non-dominated solutions with a higher C-index value when compared to the other methods MOGWO, MOMVO, and NSGA-III. This suggests that the solutions produced by MOAGWO are closer to the Pareto-optimal solutions than those produced by the other methods.

In addition, it can be seen that the C-index values for the comparison between MOAGWO and MOGWO are relatively close, with C(MOGWO, MOAGWO) having a slightly higher C-index value. Similarly, the C-index values for the comparison between MOAGWO and MOMVO are relatively close, with C(MOMVO, MOAGWO) again having a slightly higher C-index value.

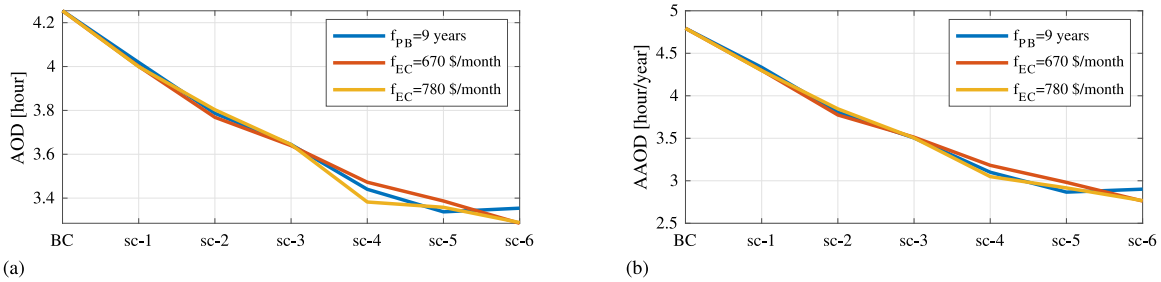

Fig. 8. (a) Average outage duration and (b) Average annual outage duration for each scenario.

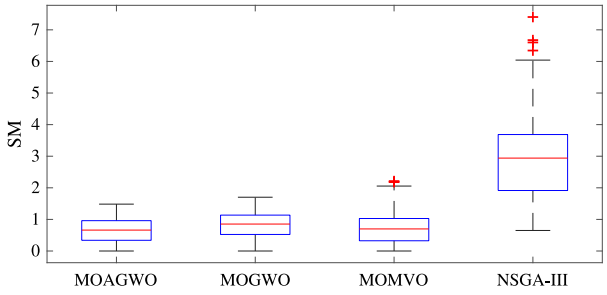

Fig. 9. The box-plots of SM values of different optimization algorithms.

Table 9
Comparisons of the algorithms using C index.

	Ave.	STD	Max.
C(MOAGWO, MOGWO)	32.5	14.2	82
C(MOGWO, MOAGWO)	34.6	13.9	79
C(MOAGWO, MOMVO)	13.3	13.4	91
C(MOMVO, MOAGWO)	29.7	15.5	85
C(MOAGWO, NSGA-III)	12.2	10.5	61
C(NSGA-III, MOAGWO)	36.3	15.7	92

On the other hand, the C-index values for the comparison between MOAGWO and NSGA-III are much further apart, with C(NSGA-III, MOAGWO) having a significantly higher C-index value. This suggests that the solutions produced by MOAGWO can significantly dominate solutions produced by NSGA-III.

Overall, these results suggest that MOAGWO is superior to the other methods with respect to C-index results (better-quality solutions within the set of non-dominated solutions). Note that the minimum C index for all comparisons was found as zero.

- The hyper-volume metric:

The HV measure is calculated by determining the volume of the region dominated by a set of solutions, bounded by a reference point. It is often used to assess the convergence and diversity of the solutions on a Pareto front, as well as to compare the performance of different algorithms.

The HV for a set of non-dominated solutions called Y (consisting of solutions y1, y2, …,yn) based on normalized values for two objective functions (f_1 and f_2), and it is defined as:

$$HV(Y,R) = volume\left(\bigcup_{i=1}^{|Y|} v_i\right) \tag{27}$$

where R is the reference point and is chosen as the maximum value for the normalized objective values. v is the hypercube whose corners are the R and all solutions in A. Higher values of HV mean that the solution set is closer to an optimal Pareto set and may also indicate a more uniform distribution of solutions in the objective space.

The Average, standard deviation, minimum, and maximum. The HV indices found for the different methods are shown in Table 10. The

Table 10
The HV values for algorithms.

	MOAGWO	MOGWO	MOMVO	NSGA-III
Ave.	0.2740	0.2740	0.2733	0.2733
STD	0.0021	0.0021	0.0023	0.0014
Min.	0.2658	0.2658	0.2627	0.2700
Max.	0.2774	0.2773	0.2767	0.2766

HV results are obtained by normalizing the objective function values and setting R to (1,1,1). Based on the results shown in Table 10, it seems that the HV values for the four algorithms (MOAGWO, MOGWO, MOMVO, and NSGA-III) are relatively similar. The average HV values for MOAGWO and MOGWO algorithms are 0.2740, slightly higher than the others. On the other hand, MOAGWO can be assigned as the best one, as it shows the highest maximum HV value for the MOGWO.

5. Summary and conclusion

This study has presented a multi-objective optimization algorithm to enhance the benefits of consumer and prosumer participation in P2P market operation in LV distribution grids. The optimal location of the modular PV panels, prosumer profits, and P2P market strategy between the consumers and prosumers are determined to minimize the payback duration for PV owners and the average monthly energy cost of the customers. The MOAGWO is used as a solution tool. Moreover, a reliability analysis using MCSs is presented to compare the load-point reliability indices across different operation scenarios. MCSs are used in the reliability analysis. The proposed methodology is applied to a 55-node European LV test feeder in six different scenarios, each representing a different number of prosumers in the system. Besides, the quality of the Pareto solutions determined by the MOAGWO is compared to those obtained by MOMVO, MOGWO, and NSGA-III by using two performance metrics.

Test system results showed that the payback duration for prosumers was around eight years for up to four prosumers in the grid and then increased for each additional PV installation. The average monthly energy cost for the customers was between 653 and 1079 USD/month. From non-dominated Pareto solutions for different scenarios, the best energy cost was found to be between 725–845 USD/month. Note that the method is not affected by the network size. Also, the proposed approach is a guide for the customers as the process is not controllable.

Load point reliability calculations were performed for some representative Pareto solutions for each scenario. It was found that adding PV units to the network generally improved the failure rate, average outage duration, and average annual outage duration. However, big improvements for the first and second PV units have decreased for the subsequent PV unit additions. That is, with the increase in the number of prosumers, there will be a saturation, which will cause an increase in the payback duration and make nearly no difference in the reliability indices, or if the payback duration is assumed constant, the energy cost will increase dramatically with nearly the same reliability indices results. So, it will not be attractive for the demand points to

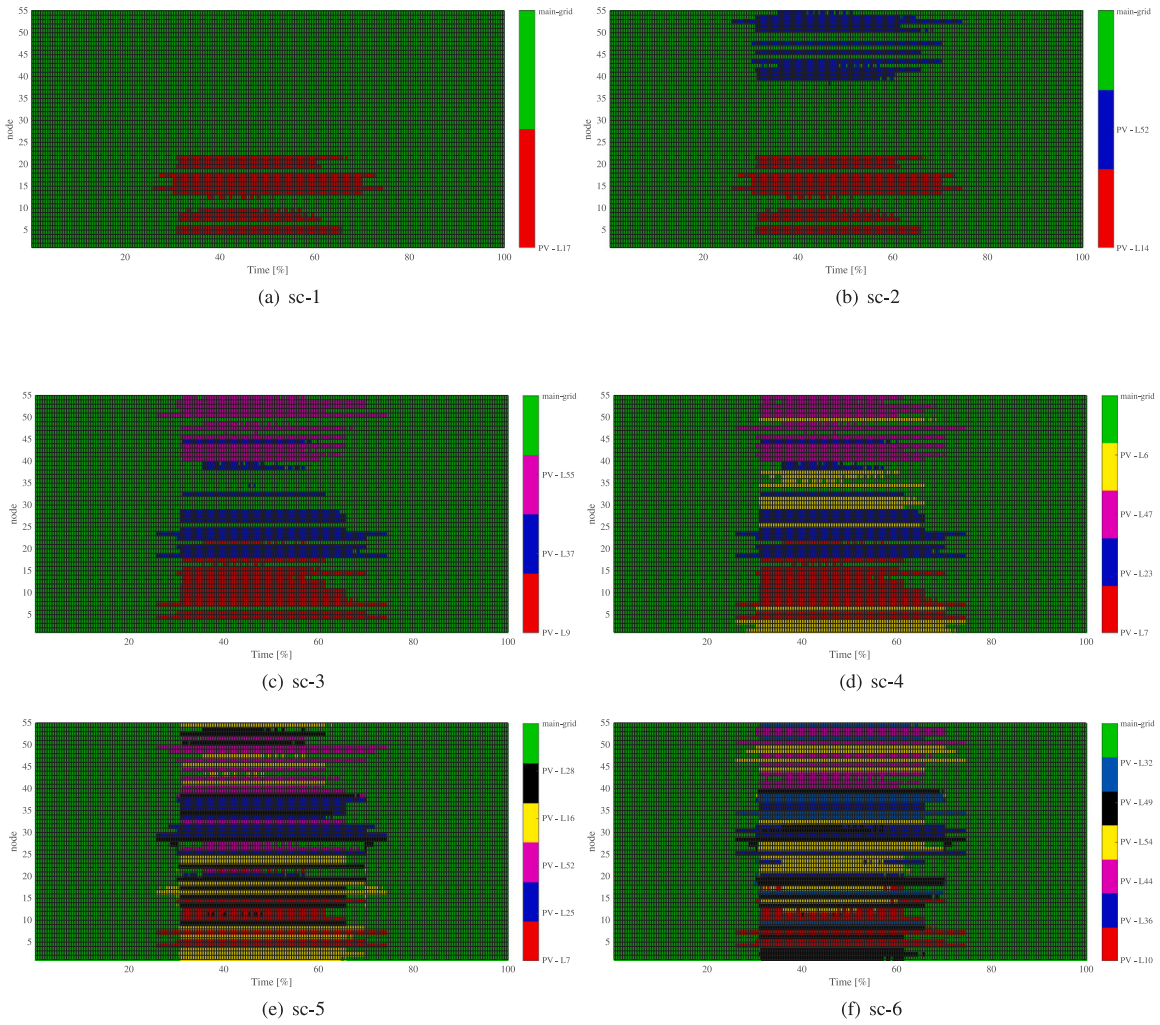

(a) sc-1 (b) sc-2

(c) sc-3 (d) sc-4

(e) sc-5 (f) sc-6

Fig. A.1. The market strategy of the system for Pareto solution with $f_{EC} = 670$ \$/month.

become prosumers as the payback duration will increase in the case of network saturation; for the consumers, as the energy cost will grow if the number of prosumers in the network increases, this situation could become a dissatisfaction reason. From Disco's point of view, on the other hand, there will not be any economic benefits, considering no impressive improvement in the energy quality and infrastructural investments postponed. If it wishes to have more prosumers in the network, DisCo or any other authorities have to provide some incentive packages for prosumers, consumers, or both.

The quality analysis of the Pareto solutions evaluated using the three multi-objective optimization metrics showed that MOAGWO and MOGWO had similar performances. They are followed by MOMVO, while NSGA-III showed the worst performance.

This study serves as a proof of concept to identify the best Pareto-optimal trade-offs between technical and economic objectives in LV distribution grids. The proposed framework will be extended to incorporate dynamic and real-time data, such as intraday variations in PV generation and demand profiles. We are also planning the accommodation of energy storage systems and electric vehicles (EVs) to investigate their impact on cost reduction, self-consumption improvement, and reliability enhancement. Another intention is to extend the proposed framework to larger and meshed LV networks to further validate its scalability. We will consider accounting for the impacts of different generation and consumption profiles depending on seasonal parameters. Finally, sensitivities for the loyalty factors and DisCo buyback prices, which are assumed to be constant, will be considered in an upcoming study.

CRediT authorship contribution statement

Keysan Polat: Software, Formal analysis, Writing – original draft, Investigation. **Bahman Ahmadi:** Conceptualization, Methodology, Writing – original draft, Software, Validation, Investigation. **Aydogan Ozdemir:** Conceptualization, Methodology, Supervision, Project administration, Writing – review & editing.

Declaration of competing interest

The authors declare that they have no known competing financial interests or personal relationships that could have appeared to influence the work reported in this paper.

Acknowledgments

This research is a part of Keysan Polat's Ph.D. thesis at Istanbul Technical University and is funded by EU HORIZON 2020 project SERENE, grant agreement No 957682.

Appendix

The optimal market strategies for the system based on candidates are shown in Figs. A.1, A.2, and A.3.

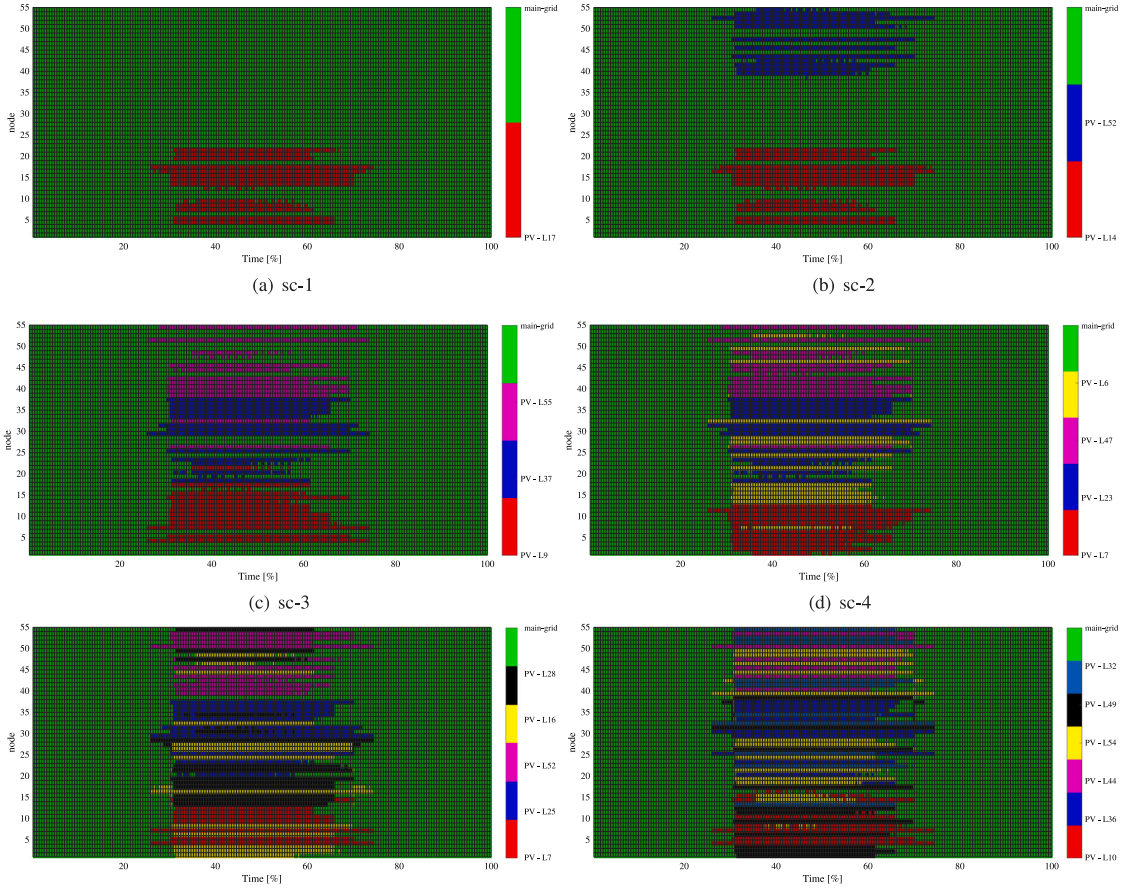

(a) sc-1 (b) sc-2

(c) sc-3 (d) sc-4

(e) sc-5 (f) sc-6

Fig. A.2. The market strategy of the system for Pareto solution with f_{EC} = 780 $/month.

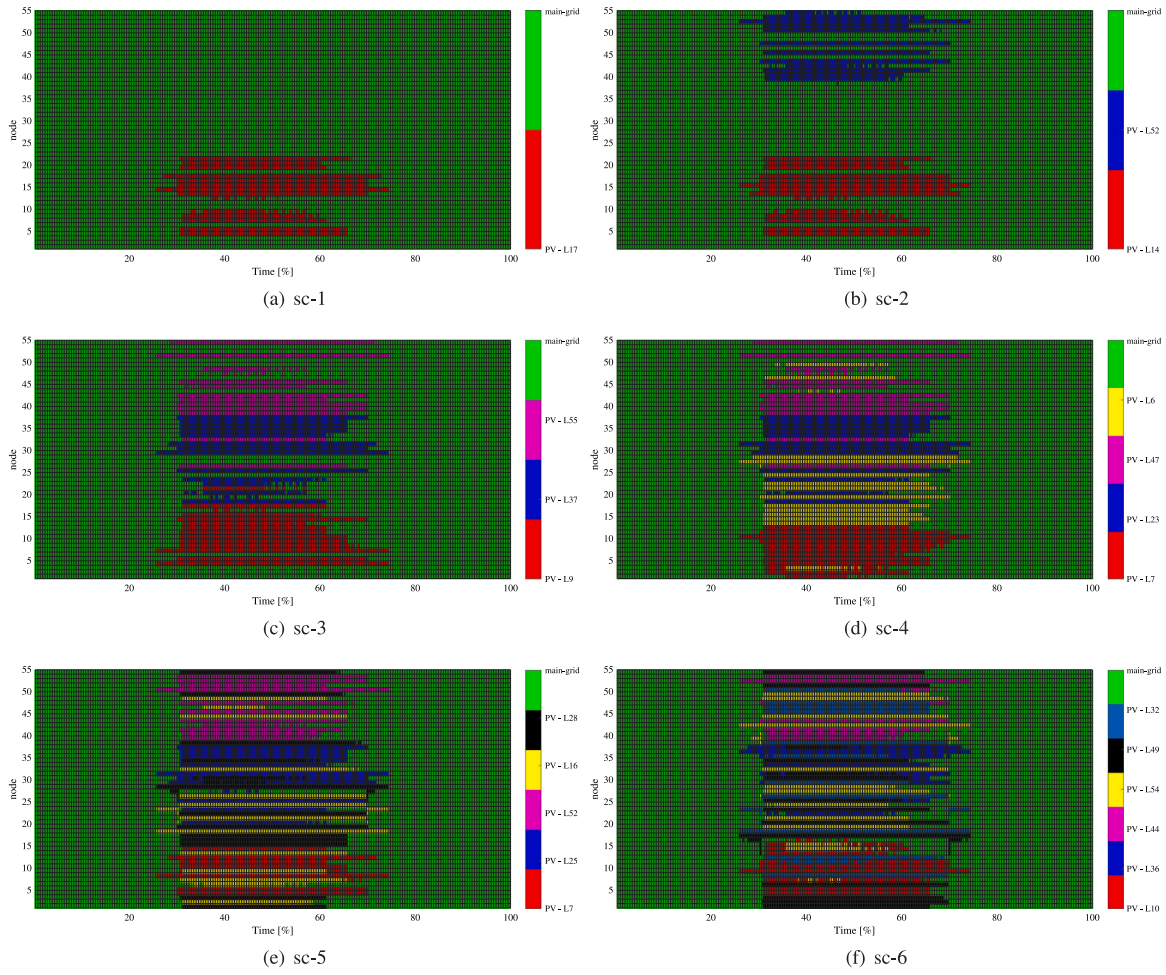

(a) sc-1 (b) sc-2

(c) sc-3 (d) sc-4

(e) sc-5 (f) sc-6

Fig. A.3. The market strategy of the system for Pareto solution with $f_{\mathrm{PB}} = 9$ years.

Data availability

Data will be made available on request.

References

[1] K. Polat, A. Ozdemir, M. Delkhooni, Reliability analysis in low voltage distribution network with peer to peer energy trading, in: 2021 IEEE Madrid PowerTech, IEEE, 2021, pp. 1–6.

[2] C. Wang, C. Liu, X. Zhou, G. Zhang, Flexibility-based expansion planning of active distribution networks considering optimal operation of multi-community integrated energy systems, Energy 307 (2024) 132601.

[3] Z. Gu, P. Li, F. Qin, X. Mai, W. Yang, H. Liu, Provincial technical loss reduction platform with interactive management and control considering reactive power compensation potential of power supply and consumption sides, Energy Rep. 11 (2024) 1846–1855.

[4] S.H.H. Dolatabadi, A. Soleimani, A. Ebtia, M. Shafie-khah, T.H. Bhuiyan, Enhancing voltage profile in islanded microgrids through hierarchical control strategies, Electr. Power Syst. Res. 231 (2024) 110270.

[5] E. Boyko, F. Byk, P. Ilyushin, L. Myshkina, K. Suslov, Methods to improve reliability and operational flexibility by integrating hybrid community mini-grids into power systems, Energy Rep. 9 (2023) 481–494.

[6] M. Alam, K. Muttaqi, D. Sutanto, An approach for online assessment of rooftop solar PV impacts on low-voltage distribution networks, IEEE Trans. Sustain. Energy 5 (2) (2013) 663–672.

[7] K. Polat, A. Ozdemir, M. Delkhooni, Load point reliability analysis in LV distribution networks with P2p energy trading, in: 2022 17th International Conference on Probabilistic Methods Applied To Power Systems, PMAPS, IEEE, 2022, pp. 1–6.

[8] P. Mochi, K.S. Pandya, R. Faia, D. Dabhi, J. Soares, Z. Vale, Empowering customers in local electricity market: A prosumer segmentation and operating envelope strategy for joint cost reduction and profit maximization, Electr. Power Syst. Res. 226 (2024) 109908.

[9] O. Jogunola, A. Ikpehai, K. Anoh, B. Adebisi, M. Hammoudeh, S.-Y. Son, G. Harris, State-of-the-art and prospects for peer-to-peer transaction-based energy system, Energies 10 (12) (2017) 2106.

[10] M.S. Javadi, A.E. Nezhad, A.R. Jordehi, M. Gough, S.F. Santos, J.P. Catalão, Transactive energy framework in multi-carrier energy hubs: A fully decentralized model, Energy 238 (2022) 121717.

[11] D. Forfia, M. Knight, R. Melton, The view from the top of the mountain: Building a community of practice with the gridwise transactive energy framework, IEEE Power Energy Mag. 14 (3) (2016) 25–33.

[12] F. Qayyum, H. Jamil, F. Jamil, D. Kim, Predictive optimization based energy cost minimization and energy sharing mechanism for peer-to-peer nanogrid network, IEEE Access 10 (2022) 23593–23604.

[13] S. Chen, C.-C. Liu, From demand response to transactive energy: state of the art, J. Mod. Power Syst. Clean Energy 5 (1) (2017) 10–19.

[14] W. Hua, J. Jiang, H. Sun, J. Wu, A blockchain based peer-to-peer trading framework integrating energy and carbon markets, Appl. Energy 279 (2020) 115539.

[15] Y. Wu, Y. Wu, H. Cimen, J.C. Vasquez, J.M. Guerrero, P2P energy trading: Blockchain-enabled P2P energy society with multi-scale flexibility services, Energy Rep. 8 (2022) 3614–3628.

[16] X. Wang, Z. Wang, Y. Mu, Y. Deng, H. Jia, Rolling horizon optimization for real-time operation of prosumers with peer-to-peer energy trading, Energy Rep. 9 (2023) 321–328.

[17] S. Zheng, X. Jin, G. Huang, A.C. Lai, Coordination of commercial prosumers with distributed demand-side flexibility in energy sharing and management system, Energy 248 (2022) 123634.

[18] L. Wang, Z. Wang, Z. Li, M. Yang, X. Cheng, Distributed optimization for network-constrained peer-to-peer energy trading among multiple microgrids under uncertainty, Int. J. Electr. Power Energy Syst. 149 (2023) 109065.

[19] R. Sepehrzad, A.S.G. Langeroudi, A. Al-Durra, A. Anvari-Moghaddam, M.S. Sadabadi, Demand response-based multi-layer peer-to-peer energy trading strategy for renewable-powered microgrids with electric vehicles, Energy 320 (2025) 135206.

[20] Y. Zhou, J. Wang, Y. Li, C. Wei, A collaborative management strategy for multi-objective optimization of sustainable distributed energy system considering cloud energy storage, Energy 280 (2023) 128183.
[21] Y. Bian, L. Xie, J. Ye, L. Ma, C. Cui, Peer-to-peer energy sharing model considering multi-objective optimal allocation of shared energy storage in a multi-microgrid system, Energy 288 (2024) 129864.
[22] Z. Guo, P. Pinson, S. Chen, Q. Yang, Z. Yang, Online optimization for real-time peer-to-peer electricity market mechanisms, IEEE Trans. Smart Grid 12 (5) (2021) 4151–4163.
[23] L. Ali, S. Muyeen, H. Bizhani, A. Ghosh, A multi-objective optimization for planning of networked microgrid using a game theory for peer-to-peer energy trading scheme, IET Gener. Transm. Distrib. 15 (24) (2021) 3423–3434.
[24] A. Hedayatnia, J. Ghafourian, R. Sepehrzad, A. Al-Durrad, A. Anvari-Moghaddam, Two-stage data-driven optimal energy management and dynamic real-time operation in networked microgrid based on a deep reinforcement learning approach, Int. J. Electr. Power Energy Syst. 160 (2024) 110142.
[25] A. Tiwari, B.K. Jha, N.M. Pindoriya, Multi-objective optimization based demand response program with network aware peer-to-peer energy sharing, Int. J. Electr. Power Energy Syst. 157 (2024) 109887.
[26] L.A. Soriano, M. Avila, P. Ponce, J. de Jesús Rubio, A. Molina, Peer-to-peer energy trades based on multi-objective optimization, Int. J. Electr. Power Energy Syst. 131 (2021) 107017.
[27] S.-M. Razavi, M.-R. Haghifam, S. Arefizadeh, S. Larimi, M. Shafie-khah, Operation of distribution network: Challenges and opportunities in the era of peer-to-peer trading, Energy Rep. 11 (2024) 4982–4997.
[28] A. El-Zonkoly, Optimal P2P based energy trading of flexible smart inter-city electric traction system and a wayside network: A case study in alexandria, Egypt, Electr. Power Syst. Res. 223 (2023) 109708.
[29] N. Saeed, F. Wen, M.Z. Afzal, Decentralized peer-to-peer energy trading in microgrids: Leveraging blockchain technology and smart contracts, Energy Rep. 12 (2024) 1753–1764.
[30] R. Sepehrzad, A. Al-Durra, A. Anvari-Moghaddam, M.S. Sadabadi, Short-term and probability scenario-oriented energy management of integrated energy distribution systems with considering energy market interactions and end-user participation, Energy 322 (2025) 135691.
[31] B. Ahmadi, S. Younesi, O. Ceylan, A. Ozdemir, An advanced grey wolf optimization algorithm and its application to planning problem in smart grids, Soft Comput. 26 (8) (2022) 3789–3808.
[32] S. Nizami, W. Tushar, M. Hossain, C. Yuen, T. Saha, H.V. Poor, Transactive energy for low voltage residential networks: A review, Appl. Energy 323 (2022) 119556.
[33] B. Ahmadi, O. Ceylan, A. Ozdemir, M. Fotuhi-Firuzabad, A multi-objective framework for distributed energy resources planning and storage management, Appl. Energy 314 (2022) 118887.
[34] S. Mirjalili, S.M. Mirjalili, A. Lewis, Grey wolf optimizer, Adv. Eng. Softw. 69 (2014) 46–61.
[35] R. Billinton, R.N. Allan, Reliability Evaluation of Power Systems, Springer Press, 1996.
[36] K. Polat, A. Ozdemir, Impacts of transactive energy trading on the load point reliability indices of LV distribution system, IEEE Access 11 (2023) 132119–132130.
[37] European L.V. Test Feeder, 2017, http://ewh.ieee.org/soc/pes/dsacom/testfeeders/European_LV_Test_Feeder.zip/ (accessed 19 November 2022).
[38] B. Ahmadi, Load-DG DATA needed for LV and MV distribution grids, 2023, https://github.com/bahman-ahmadi-aso/load_DG_DATA.
[39] B. Ahmadi, A. Pappu, G. Hoogsteen, J.L. Hurink, Multi-objective optimization framework for integration of distributed energy resources in smart communities, in: 2022 57th International Universities Power Engineering Conference, UPEC, IEEE, 2022, pp. 1–6.
[40] EMRA Billing Base Prices, 2022, https://www.epdk.gov.tr/Detay/Icerik/3-1327/elektrik-faturalarina-esas-tarife-tablolari (Accessed 19 November 2022).
[41] BEDAS Annual Report, 2019, https://www.bedas.com.tr/UserFiles/File/Faaliyet_Raporu_2019.pdf (Accessed 19 November 2022).
[42] S. Mirjalili, P. Jangir, S.Z. Mirjalili, S. Saremi, I.N. Trivedi, Optimization of problems with multiple objectives using the multi-verse optimization algorithm, Knowl.-Based Syst. 134 (2017) 50–71.
[43] S. Mirjalili, S. Saremi, S.M. Mirjalili, L.d.S. Coelho, Multi-objective grey wolf optimizer: a novel algorithm for multi-criterion optimization, Expert Syst. Appl. 47 (2016) 106–119.
[44] J.-H. Yi, S. Deb, J. Dong, A.H. Alavi, G.-G. Wang, An improved NSGA-III algorithm with adaptive mutation operator for big data optimization problems, Future Gener. Comput. Syst. 88 (2018) 571–585.